A hybrid modeling framework for city-scale dynamics of multi-strain influenza epidemics [*]

Vasiliy Leonenko[1][0000−0001−7070−6584]

ITMO University, 49 Kronverksky Pr., St. Petersburg, Russia 197101
vnleonenko@yandex.ru

Abstract. In the current paper we present a hybrid modeling framework which allows to simulate co-circulation of influenza strains in urban settings. It comprises a detailed agent–based model coupled with SEIR-type compartmental model. While the former makes it possible to simulate the initial phase of an outbreak when the heterogeneity of the contact network is crucial, the latter approximates the disease dynamics after the occurrence of mass infection thus dramatically increasing the framework performance. The numerical experiments with the model are presented and their results are discussed.

Keywords: Python · influenza · co-circulation · agent-based models · compartmental models

1 Introduction

Outbreaks of influenza, one of the oldest and the most widely spread human infectious diseases, result in 3 to 5 million cases of severe illness annually worldwide, and the mortality rate is from 250 to 640 thousand individuals per year [15]. In addition to induced mortality, influenza causes an increase of heart attacks and strokes [6], as well as other disease complications. To enhance the capabilities of influenza surveillance and, as a consequence, to find means of restraining influenza epidemics and reducing the mortality attributed to influenza complications, the healthcare organs widely use statistical and mechanistic models. Among the factors of influenza dynamics, that are considered influential and thus should be included into the models, are contact patterns in the population [1], [22], [20], [30], and the immunity levels to various influenza strains [2], [12], [17], [27]. The latter is connected with the former, as the heterogeneity of networks of disease transmission might cause uneven distribution of the infected and consequently the immune people, leading to intricate prevalence dynamics and the inability of simple models to predict it. As an example, in a deterministic SEIR model it is assumed that the population immunity level directly defines the outbreak incidence dynamics and ultimately the outbreak size. At the same

---

time, is it known that in real life the infection prevalence dynamics is very dependent on the stochastic effects inherent to the initial stages of the epidemic onset and the contact network clustering [5], [9].

The modeling technique which makes it possible to account for the influence of contact network heterogeneity on the disease transmission is multi-agent modeling. There is a number of known publications on the topic, including such articles as [21], where multi-agent modeling of vaccination scenarios in heterogeneous populations based on social network incidence data. Another examples include a multi-component stochastic model that reproduces the dynamics of influenza in certain regions of England and Wales for 14 years [2] and the works of research teams that use a multi-agent approach to predict the dynamics of influenza based on synthetic populations — these are the teams of the University Pittsburgh ([19], [20], [28]), RTI International [7], [8], and Wake Forest University School of Medicine [11]. The same concept was recently applied to COVID-19 modeling, with the examples such as COVASIM [16], [18]. The author of this article employed an agent-based model to replicate the 2010–2011 outbreak in St Petersburg by means of the synthetic population of this city [22], [24] and analyzed the co-circulation of several influenza strains in the same population depending on the initial immunity levels [26].

One of the main drawbacks of the multi-agent approach which seriously limits its application is related to excessive demand of computational power to handle the experiments with the model. Even in the simplest case, when the aim is to calculate the disease trajectory for one outbreak at the city scale with a predefined set of parameter values, several simulation runs are required to address stochastic uncertainty. As a result, the experiment may last from hours to days, depending on the model employed and the computational resources available. Obviously, in these circumstances the tasks which require many repetitive launches with different parameter values, such as model calibration to data or uncertainty/sensitivity analysis, may not be performed in reasonable time. There exist different methods to overcome this obstacle, namely, those related to preliminary data modification (for example, using a representative sample of individuals rather than the whole population in the simulations), to algorithm optimization and parallel computing (particularly, GPGPU-compatible framework implementations), and to simplification of some of the processes within the dynamics of the regarded system (for instance, by training neural networks on the output of multi-agent models to replicate disease incidence and prevalence trajectories without actual simulation). Among the last group of approaches hybrid modeling of disease dynamics can be named [4], [14], [13]. The mentioned method is based on the idea that in some sets of conditions the difference in the outputs of the detailed multi-agent models and much simpler compartmental ones may be negligible [29] which makes it possible to locally replace the former approach by the latter without dramatic loss of disease dynamic reproduction accuracy. With the mentioned benefits come the drawbacks. Particularly, the necessity of using two different modeling techniques for describing a single infection process instance raises a question of compatibility of those techniques. How

smooth the transitions between the two models are and what is the influence of switching condition on the regarded disease dynamics? We try to address these questions in the current study, using a created hybrid modeling framework which allows to replicate artificial outbreaks caused by co-circulation of influenza strains in a synthetic population. To the author's knowledge, it is the first attempt of hybrid simulation of virus co-circulation. The presented study is a part of the ongoing research, the ultimate aim of which consists in quantifying the interplay between the immunity formation dynamics and the circulation of influenza strains in Russian cities. The study results are also applicable to modeling the circulation of arbitrary acute respiratory infections, particularly, COVID-19.

2   Methods

2.1   The multi-agent model

Overall description. The original model used as a base for the framework is an agent-based model of co-circulation of different influenza strains in a synthetic population which is described in detail in [26]. It has discrete time with the modeling step equal to one day. The epidemic process is initiated by assigning randomly an infectious status to some individuals in the synthetic population at the beginning of the simulation. The model output includes generation of spatial distributions of the incidence cases via independent simulation runs, calculation of cumulative incidence and prevalence in the area under study and assessing the levels of herd immunity in the population after the outbreak. It is possible to collect additional data, such as places of infection (school, workplace, home and its immediate vicinity) for each incidence case, which allows to assess the contribution of contacts in each type of place to the spread of infection.

Population. The population-related parameters used for the model are organized in a form of a synthetic population of St Petersburg for the year 2010. The population includes 40213 households with the cumulative number of dwellers being 4,865,118 individuals. The residential buildings are regarded as a bunch of separate dwellings, and the individual can contact only with the people they share a dwelling with (e.g, with family members). Following the statistics of the governmental service "Open data of Saint Petersburg" [10], the average number of people per dwelling as 2.57, which is used as a mean for the generation of number of dwellers in each household (Poisson distribution is employed). We assumed that all the young people aged 7 to 17 attend schools, and the adults of working age (18 to 55 for males and 18 to 60 for females) can work. The workplaces are split into small compartments within which the daily contacts occur. The average workplace size was chosen equal to the average daily number of workplace contacts. We generate the workplace compartment sizes using the Poisson distribution with the corresponding mean. We consider that workplaces for the adults and schools for the school–age children are selected randomly from

the available positions within a certain radius from the household (based on general knowledge, we took 15 km and 5 km correspondingly, which seems adequate for St Petersburg). If there are no vacancies in schools/vacant workplaces within this radius, the closest vacancy is assigned disregarding the distance. The remained individuals without schools are assigned to closest schools in disregard of the school capacity, while the remained individuals without workplaces are considered jobless.

Contacts. We assume that there exist the following patterns of a daily activity depending on the individual:

- stay in the household with a fixed `id` during the whole day (pre–school children, retired, unemployed)
- go to the school with a fixed `id` (students)
- go to the workplace with the particular `id` (working adults)

Hence, each day one individual has 1 to 2 places of potential contacts which are not changed over time. The contact numbers were derived from the data used by the author in the compartmental influenza model for St. Petersburg [23]. These data were calculated from the contact matrices for Russian cities [1]. We assumed that, in average, the dwellers of St. Petersburg have 1.57 contacts within the household and 8.5 outside it (at school or at work, which are mutually exclusive). Taking into account the differences in activity patterns of people (some of them do not work or study), the average calculated number of daily contacts in a model is around 6.51, which is close to the average number introduced in [23] (6.528). The role of public transport in spreading the infection is not considered. In the current version of the framework, the weekends are not regarded separately, i.e. the behavior of the individuals is the same during all the days.

Disease onset and recovery. The rate of effective contacts in a particular activity location (that is, the contacts between a susceptible and an infected individual which result in new infection cases) depends on the average number of contacts per person per day and the infection transmission coefficient, which are parameters of the model. We take a simplifying assumption that the infection transmission coefficients are not dependent on the strain. If various strains are instantaneously transmitted to an individual at the place of contact, one of them is selected at random as the one causing the infection. Each agent in the population potentially interacts with other agents if they attend the same school (for schoolchildren), workplace (for working age adults), or lives in the same household.

The infectivity of each individual depends on their day of infection. The fraction of infectious individuals in the group of individuals infected τ days before the current moment t is defined by a piecewise constant function g_τ which reflects the change of individual infectiousness over time from the moment of acquiring

influenza. It is assumed that there exists some moment $\bar{t}$: $\forall t \geq \bar{t}$ $g_\tau = 0$, which corresponds to the moment of recovery. The values of $g(\tau)$ were set according to [3], with τ measured in days: $g(0) = g(1) = 0$, $g(2) = 0.9$, $g(3) = 0.9$, $g(4) = 0.55$, $g(5) = 0.3$, $g(6) = 0.15$, $g(7) = 0.05$, $g(8) = g(9) = \cdots = 0$. We assume that the fraction of infectious individuals over time is not dependent on the strain. Individuals recovered from the disease are considered immune to the particular influenza strain, that caused it, until the end of the simulation. Cross-immunity is not considered, i.e. the mentioned recovered individuals do not acquire immunity to other influenza strains.

Parameter name	Description	Value
α_m	A fraction of the individuals which are non-immune to the virus strain m	$\{0.78,\quad 0.74, 0.6\}$ [26]
λ	Infection transmission coefficient	0.3 [26]
c_{sch}	Average daily number of contacts in schools	8.5
c_{wp}	Average daily number of contacts in workplaces	8.5
c_{hh}	Average daily number of contacts in households	1.57
$I_0^{(m)}$	Initial number of individuals infected by a given strain m	5

Table 1. Multi-agent model parameters

2.2   The compartmental model

As a simplified substitute for the multi-agent model, a multi-strain compartmental model is used based on a deterministic system of difference equations, with the time step equal to one day. The thorough model description can be found in [25]. Analogous to a multi-agent model, we consider the co-circulation of three influenza strains, A(H1N1)pdm09, A(H3N2) and B, thus, we assume $n_s = 3$, where n_s is the total number of regarded strains. Different strains of influenza B type are not distinguished and the dominant B type strain is regarded during each epidemic season. Let $x_t^{(h)}$ be the fraction of susceptible individuals in the population with exposure history $h \in \overline{1, n_s + 1}$, $y_t^{(m)}$ be the number of individuals newly infected at the moment t by the virus strain m and $\overline{y}_t^{(m)}$ – the cumulative number of infectious persons by the time t transmitting the virus strain m, $m \in \overline{1, n_s}$. A possibility of co-infection by multiple strains in the course of one season is not regarded, hence, the individuals recovered from the influenza caused by any of the circulating strains are considered immune. However, this assumed cross-immunity between virus strains is not transferred to the next epidemic season.

The susceptible individuals are divided into subgroups based on their exposure history h, $h \in \overline{1, n_s + 1}$. A group of susceptible individuals with exposure history state $h \in \overline{1, n_s}$ is composed of those individuals who were subjected to infection by the strain m in the previous epidemic season, whereas a group with exposure history state $h = n_s + 1$ is regarded as naive to the infection caused by any strain. The variable $\mu \in [0; 1)$ reflects the fraction of population which do not participate in infection transmission. In the default case, $\mu = 0$. Due to immunity waning, the individuals with the history of exposure to a fixed influenza strain in the preceding season might lose immunity to the same strain in the following epidemic season. We assume that the fraction a of those individuals, $a \in (0; 1)$, becomes susceptible, whereas $1 - a$ individuals retain their immunity during the modeled epidemic season. As a result, a function $f(h, m)$ is introduced into the model which defines the proportion of the individuals with exposure history state h, who are susceptible to virus strain m:

$$f(h, m) = \begin{cases} a, & m = h, \\ 1, & m \neq h. \end{cases} \tag{1}$$

The modeling equation system is formulated in the following way:

$$x_{t+1}^{(h)} = \max \left\{ 0, \left(1 - \sum_{m=1}^{n_s} \frac{\beta^{(m)}}{\rho} \overline{y}_t^{(m)} f(h, m) \right) x_t^{(h)} \right\}, h \in \overline{1, n_s + 1}, \tag{2}$$

$$y_{t+1}^{(m)} = \frac{\beta^{(m)}}{\rho} \overline{y}_t^{(m)} \sum_{h=1}^{n_s + 1} f(h, m) x_t^{(h)}, m \in \overline{1, n_s},$$

$$\overline{y}_t^{(m)} = \sum_{\tau=0}^{T} y_{t-\tau}^{(m)} g_\tau^{(m)}, m \in \overline{1, n_s},$$

$$x_0^{(h)} = \alpha^{(h)}((1 - \mu)\rho - \sum_{m=1}^{n_s} y_0^{(m)}) \geq 0, h \in \overline{1, n_s + 1},$$

$$y_0^{(m)} = \varphi_0^{(m)} \geq 0, m \in \overline{1, n_s}. \tag{3}$$

The piecewise constant function g_τ gives a fraction of infectious individuals in the group of individuals infected τ days before the current moment t and is defined in the same way as in the multi-agent model. An intricate model of contacts in a synthetic population is replaced by a mass action law with the intensity of effective contacts $\beta^{(m)}$, defined separately for each influenza strain m:

$$\beta^{(m)} = \lambda^{(m)} \delta,$$

where $\lambda^{(m)}$ is virulence of the strain m, δ is the average number of contacts in the population [23].

While in the original model from [25] it was assumed that all the initially infected individuals are in their first infective day (for the employed $g(\tau)$ it is the day 2 after the infection), the compartmental submodel from this study is able to

handle the disease prehistory, i.e. the initially infected people are distinguished by the day of their infection. The number of infected is transferred from the multi-agent model at the moment of switching.

Variable	Description	Values
ρ	Population size, people	$4,865,118$
$\alpha^{(h)}$	A fraction of population exposed to the strain m in the preceding epidemic season, $h \in \overline{1,m}$	$\{0.78, 0.74, 0.6\}$
$\lambda^{(m)}$	Virulence of the virus strain m	0.3
a	The fraction of people who lost immunity after being exposed to the virus strain in the preceding epidemic season	0.3 [25]
δ	Average daily number of contacts in the population for a fixed individual	6.528 [23]

**Table 2.** Compartmental model parameters

2.3 Switching algorithm

One of the important aspects of a hybrid modeling is to properly decide how to define the switching conditions, when a detailed multi-agent model should be replaced by a compartmental model during a simulation run. As it can be seen from Figure 1, the calculation time for a single algorithm step (a modeling day) is growing very fast with the step number due to the increase in the number of infected people in the population. Thus, it is beneficial to approximate the infection process by a simpler model starting from the moment, when the number of infected people becomes large.

In [4] two switching condition types were proposed:

- Switch to a compartmental model when a certain number of infected individuals in the population is reached;
- Switch to a compartmental model when the effective reproduction number of the infection is stabilized (the difference between the corresponding values for the subsequent simulation days becomes lower than a certain threshold).

While both switching conditions are quite effective and interpretable in the case of a disease dynamics caused by a single virus, they cannot be easily adopted for our case due to the existence of multiple viruses in the population. The typical situation in virus co-circulation modeling corresponds to high prevalence caused by one strain and low prevalence caused by other strains. As a result, if we make a switch based on the cumulative numbers of the infected people or the cumulative reproduction number, the disease dynamics of the virus with low prevalence might be altered compared to the original model. On the other hand, if the switch is to be performed when the threshold is reached by the
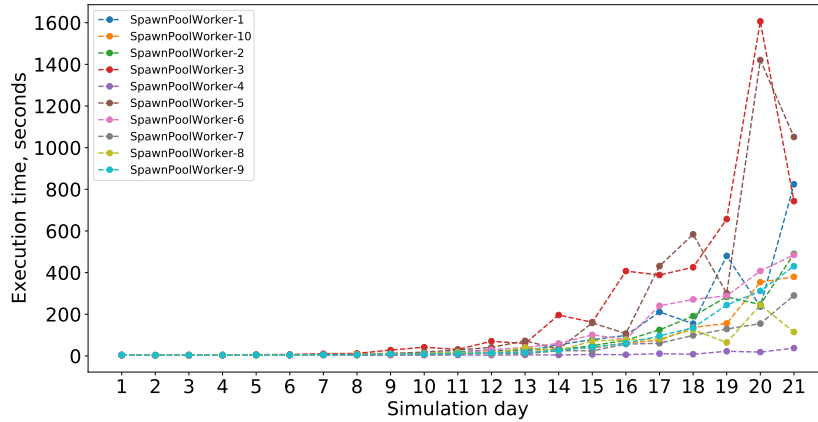
Fig. 1. Calculation time for a single time step depending on the simulation day.

rarest strain's infection number, it will lead to no switching at all or to the late switching, because minor epidemics with the prevalence never exceeding a threshold are typical for almost every simulation run.

In this study, we perform numerical experiments with a hybrid model based on a time-related switching condition, i.e. the moment of the switch is tied to the simulation day. Table 3 contains execution time corresponding to simulation runs from Section 3.1. The table demonstrates that earlier switching gives an immense economy of execution time. In fact, the share of computational time for the compartmental submodel in the overall simulation process might be considered negligible, because it is much faster than its multi-agent counterpart, thus, the hybrid simulation with the switching moment t^* is very close in computation time to performing t^* time steps of the original multi-agent model.

Moment of switching, t^*	5	10	15	20
Execution time, seconds	267.6	1185.5	4748.5	131784.8

Table 3. Hybrid modeling algorithm performance

A crucial aspect of the switching is to ensure that the parameters of both submodels align, otherwise instead of a single simulated prevalence trajectory with varied level of detail we might obtain two independent epidemic processes. In Table 4, the parameter matching is described.

As it is clear from the table, the following two parameters are the main source of potential bias between the outputs of the two submodels:

– Average daily number of contacts δ. Obviously, the contact process in the compartmental model lacks much detail compared to the explicit modeling

Variable	Description	Compatibility between submodels
ρ	Population size, people	Equivalent
$\alpha^{(h)}$	A fraction of population exposed to the strain m in the preceding epidemic season, $h \in \overline{1, m}*$	Equivalent
$\lambda^{(m)}$	Virulence of the virus strain m	Equivalent
a	A fraction of people who lost immunity after being exposed to the virus strain in the preceding epidemic season	Equivalent
δ	Average daily number of contacts in the population for a fixed individual	Matched by averaging
μ	A fraction of the individuals with the protection from infection by any influenza strains	Population submodel only

Table 4. Parameter compatibility between the submodels

of the contacts in a synthetic population, thus even if the average number of contacts is correctly calculated from the corresponding multi-agent submodel data, the discrepancy in the actual number of contacts is inevitable.

– A fraction μ of the individuals with the protection from infection by any influenza strains. This parameter was somewhat artificially added to a model to make it possible to calibrate the compartmental model to real data. In [25] it was shown that with $\mu = 0$, when all the individuals without expection are prone to the infection, the compartmental model gives implausible prevalence curves — they are either too high (unrealistic epidemic intensity) or too wide (unrealistic epidemic duration) compared to the real observed epidemic outbreaks. We assumed thus that μ is dependent on the fraction of cases which is missed in the statistics due to under-reporting (hence, lower prevalence peaks in data) and also on the topology of the contact network (unlike it is assumed in SEIR-type compartmental models, not all of the individuals participate in the epidemic transmission).

The analysis of the dependence of hybrid model output on t^* and μ was performed in the numerical experiments described in the following section.

3   Simulation

The simulation framework implementing the described hybrid model was developed using Python 3.8 programming language. The simulation runs were executed in parallel using `multiprocessing` library. The hardware used was Intel Xeon cluster with 24 virtual (12 physical) cores. A single experiment included 10–20 repetitive simulation runs. The result of one experiment is thus 30–60 trajectories in total (10–20 for each of three co-circulating influenza strains).

3.1   Switching moment influence

The first set of experiments with the hybrid model was conducted to compare prevalence trajectories obtained with different values of t^*. The value $\mu = 0.9$ was set based on the previous experience of compartmental model calibration [25]. On the Figure 2 below, from left to right in a fixed row one can see output prevalence curves for three circulating virus strains. From top to bottom, it is shown how the output corresponding to a fixed virus strain changes depending on the input parameters. The moment of switching is shown on each graph by a gray dotted line.

Figure 2 shows that the resulting output is generally similar throughout the experiments, however, there exists a visible increase in the maximum total number of infected individuals with the increase of t^* (the images top to bottom for a fixed strain). Also, the very moment of the switch is clearly visible on the graphs, which indicates that the submodel matching by simple equaling of the parameter values does not allow for smooth transition. Thus the framework might require modifications to assure correct coupling of the submodels. That observation is coherent with the findings demonstrated by other research groups [29].
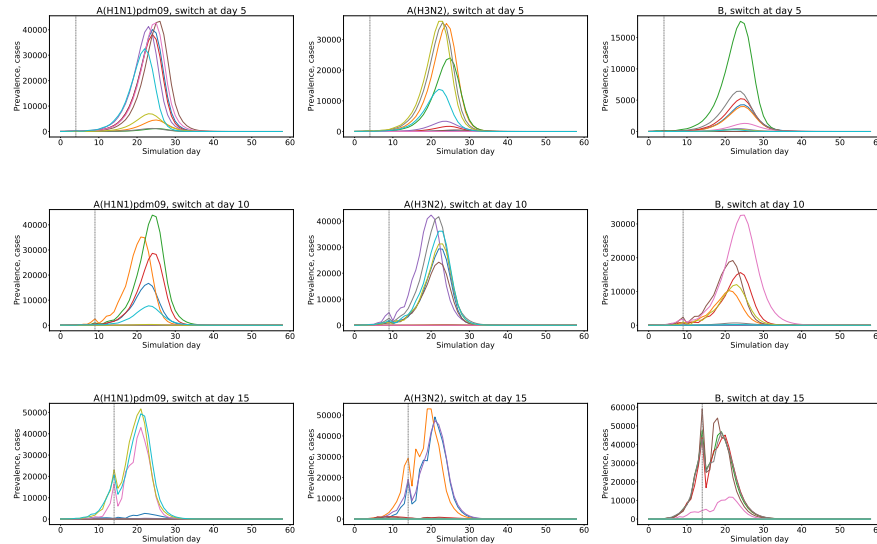
Fig. 2. Prevalence dynamics for different switching moments t^*, the fraction of protected individuals $\mu = 0.9$ set according to [25]. A row of three figures corresponds to an output of a single experiment while a column shows the comparative prevalence of infection caused by one virus strain depending on t^*.

3.2   Protected individuals fraction influence

The second set of experiments with the hybrid model was conducted to find out how the value of μ might influence the resulting output.
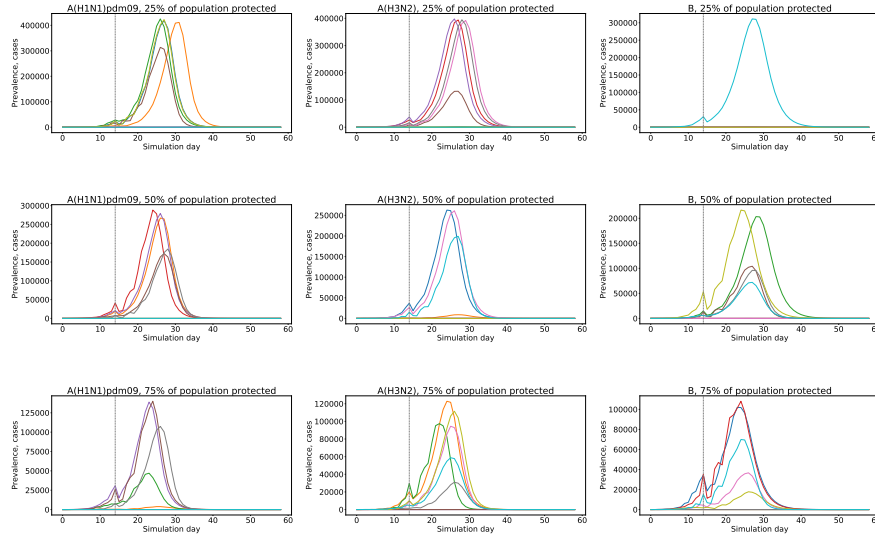
Fig. 3. Incidence dynamics depending on the fraction of protected individuals μ.

Figure 3 demonstrates that changing μ indeed alters dramatically the maximum prevalence. Thus, to ensure the plausibility of the hybrid model output, the value of μ for the compartmental submodel should be somehow calibrated to real data and/or aligned with the properties of the contact structure used in the multi-agent submodel.

4   Conclusions

In this article, the structure of the hybrid modeling framework is presented which allows to find a good trade-off between the output detail and the computational speed. Also, several experiments were conducted and demonstrated which aimed at preliminary investigation of the applicability of the introduced concept. The following conclusions might be made based on the results:

- The usage of the hybrid model makes it possible to calculate prevalence trajectories much faster than using the original multi-agent model (see Table 3), and to add more detail to the disease transmission description (e.g., by considering supermarkets and public transport as potential places of contacts). However, since the choice of the switching moment t^* alters the output, and,

obviously, the switch made too early renders a multi-agent component of the hybrid network useless, the problem of careful selection of this value should be properly addressed in the forthcoming research. One of the things which is to be done in that direction is to compare the presented outputs of the hybrid model with the output of the original multi-agent model and to assess how fast the bias between the trajectories decreases with the increase of t^*. This investigation will make it possible to find a dependence between the output accuracy and the simulation execution time under a fixed set of input parameters.

– The demonstrated discontinuity of prevalence trajectories at the moment of switching calls for refining the switching algorithm. Particularly, it is necessary to establish whether this problem arises due to incompatibility of modeling structures or poor matching of parameter values. According to [29], while there is an equivalence between the averaged and network model, the parameters still need to be adjusted. Since the networks are not homogeneous, one needs to calculate the revised "effective" value of disease transmission intensity. This approach, along with the switching based on stabilized transmission detection, will be implemented in the near future.

– The presence of the parameter μ in the compartmental submodel, which does not have a clear interpretation, complicates the alignment of the two submodels. A possible solution of the issue is to find a way how to derive the value of μ from real data or from the parameter values of the multi-agent submodel. Since this result might be obtained only after clarifying the parameter meaning, a full-fledged separate research is required.

– In the current article, separate trajectories were shown on the graphs, since the aim was to demonstrate how a given trajectory behaves before and after switching the submodels. However, for the practical aims of using the hybrid modeling framework, particularly, for the calibration to real data and for the uncertainty analysis, the confidence intervals should be assessed and compared depending on switching moment t^*. That will allow to understand how the usage of the hybrid model alters the uncertainty of the prevalence estimation compared to the original multi-agent framework.

The author believes that the mentioned steps will make the described hybrid modeling framework a valueable tool for short-term infection prediction of influenza and COVID-19 prevalence, along with the analysis of their possible co-circulation, which is stated to pose potential danger for the population well-being.

References

1. Ajelli, M., Litvinova, M.: Estimating contact patterns relevant to the spread of infectious diseases in Russia. Journal of Theoretical Biology **419**, 1–7 (2017)
2. Baguelin, M., Flasche, S., Camacho, A., Demiris, N., Miller, E., Edmunds, W.J.: Assessing optimal target populations for influenza vaccination programmes: an evidence synthesis and modelling study. PLoS medicine **10**(10), e1001527 (2013)

 3. Baroyan, O., Basilevsky, U., Ermakov, V., Frank, K., Rvachev, L., Shashkov, V.: Computer modelling of influenza epidemics for large-scale systems of cities and territories. In: Proc. WHO Symposium on Quantitative Epidemiology, Moscow (1970)
 4. Bobashev, G.V., Goedecke, D.M., Yu, F., Epstein, J.M.: A hybrid epidemic model: combining the advantages of agent-based and equation-based approaches. In: 2007 winter simulation conference. pp. 1532–1537. IEEE (2007)
 5. Brett, T., Ajelli, M., Liu, Q.H., Krauland, M.G., Grefenstette, J.J., van Panhuis, W.G., Vespignani, A., Drake, J.M., Rohani, P.: Detecting critical slowing down in high-dimensional epidemiological systems. PLOS Computational Biology **16**(3), 1–19 (03 2020)
 6. CDC: People with heart disease and those who have had a stroke are at high risk of developing complications from influenza (the flu). [online], http://www.cdc.gov/flu/heartdisease/
 7. Cooley, P., Brown, S., Cajka, J., Chasteen, B., Ganapathi, L., Grefenstette, J., Hollingsworth, C.R., Lee, B.Y., Levine, B., Wheaton, W.D., et al.: The role of subway travel in an influenza epidemic: a New York City simulation. Journal of Urban Health **88**(5), 982 (2011)
 8. Cooley, P.C., Bartsch, S.M., Brown, S.T., Wheaton, W.D., Wagener, D.K., Lee, B.Y.: Weekends as social distancing and their effect on the spread of influenza. Computational and Mathematical Organization Theory **22**(1), 71–87 (2016)
 9. Drake, J.M., Brett, T.S., Chen, S., Epureanu, B.I., Ferrari, M.J., Marty, E., Miller, P.B., O'Dea, E.B., O'Regan, S.M., Park, A.W., Rohani, P.: The statistics of epidemic transitions. PLOS Computational Biology **15**(5), 1–14 (05 2019)
10. Government of Saint Petersburg: Otkritie dannie Sankt-Peterburga [Open data of Saint-Petersburg], https://data.gov.spb.ru/opendata/7840013199-passports_houses/versions/9/ (In Russian.) Last visited: 04/19/2020.
11. Guo, D., Li, K.C., Peters, T.R., Snively, B.M., Poehling, K.A., Zhou, X.: Multi-scale modeling for the transmission of influenza and the evaluation of interventions toward it. Scientific reports **5**(1), 1–9 (2015)
12. Hill, E.M., Petrou, S., De Lusignan, S., Yonova, I., Keeling, M.J.: Seasonal influenza: Modelling approaches to capture immunity propagation. PLoS computational biology **15**(10), e1007096 (2019)
13. Hunter, E., Kelleher, J.D.: Adapting an agent-based model of infectious disease spread in an irish county to covid-19. Systems **9**(2), 41 (2021)
14. Hunter, E., Mac Namee, B., Kelleher, J.: A hybrid agent-based and equation based model for the spread of infectious diseases. Journal of Artificial Societies and Social Simulation **23**(4) (2020)
15. Iuliano, A.D., Roguski, K.M., Chang, H.H., Muscatello, D.J., Palekar, R., Tempia, S., Cohen, C., Gran, J.M., Schanzer, D., Cowling, B.J., et al.: Estimates of global seasonal influenza-associated respiratory mortality: a modelling study. The Lancet **391**(10127), 1285–1300 (2018)
16. Kerr, C.C., Stuart, R.M., Mistry, D., Abeysuriya, R.G., Rosenfeld, K., Hart, G.R., Núñez, R.C., Cohen, J.A., Selvaraj, P., Hagedorn, B., et al.: Covasim: an agent-based model of covid-19 dynamics and interventions. PLOS Computational Biology **17**(7), e1009149 (2021)
17. Konshina, O., Sominina, A., Smorodintseva, E., Stolyarov, K., Nikonorov, I.: Population immunity to influenza virus A(H1N1)pdm09, A(H3N2) and B in the adult population of the Russian Federation long-term research results. Russian Journal of Infection and Immunity **7**(1), 27–33 (2017). https://doi.org/10.15789/2220-7619-2017-1-27-33, in Russian.

18. Krivorotko, O., Sosnovskaia, M., Vashchenko, I., Kerr, C., Lesnic, D.: Agent-based modeling of covid-19 outbreaks for new york state and uk: Parameter identification algorithm. Infectious Disease Modelling **7**(1), 30–44 (2022)
19. Kumar, S., Grefenstette, J.J., Galloway, D., Albert, S.M., Burke, D.S.: Policies to reduce influenza in the workplace: impact assessments using an agent-based model. American journal of public health **103**(8), 1406–1411 (2013)
20. Kumar, S., Piper, K., Galloway, D.D., Hadler, J.L., Grefenstette, J.J.: Is population structure sufficient to generate area-level inequalities in influenza rates? an examination using agent-based models. BMC public health **15**(1), 947 (2015)
21. Lee, B.Y., Brown, S.T., Korch, G.W., Cooley, P.C., Zimmerman, R.K., Wheaton, W.D., Zimmer, S.M., Grefenstette, J.J., Bailey, R.R., Assi, T.M., et al.: A computer simulation of vaccine prioritization, allocation, and rationing during the 2009 h1n1 influenza pandemic. Vaccine **28**(31), 4875–4879 (2010)
22. Leonenko, V., Arzamastsev, S., Bobashev, G.: Contact patterns and influenza outbreaks in Russian cities: A proof-of-concept study via agent-based modeling. Journal of Computational Science **44**, 101156 (2020)
23. Leonenko, V., Bobashev, G.: Analyzing influenza outbreaks in Russia using an age-structured dynamic transmission model. Epidemics **29**, 100358 (December 2019)
24. Leonenko, V., Lobachev, A., Bobashev, G.: Spatial modeling of influenza outbreaks in Saint Petersburg using synthetic populations. In: International Conference on Computational Science. pp. 492–505. Springer (2019)
25. Leonenko, V.N.: Herd immunity levels and multi-strain influenza epidemics in russia: a modelling study. Russian Journal of Numerical Analysis and Mathematical Modelling **36**(5), 279–291 (2021)
26. Leonenko, V.N.: Modeling co-circulation of influenza strains in heterogeneous urban populations: the role of herd immunity and uncertainty factors. In: International Conference on Computational Science. pp. 663–669. Springer (2021)
27. Leonenko, V.N., Danilenko, D.M.: Modeling the dynamics of population immunity to influenza in Russian cities. ITM Web of Conferences **31**, 03001 (2020)
28. Lukens, S., DePasse, J., Rosenfeld, R., Ghedin, E., Mochan, E., Brown, S.T., Grefenstette, J., Burke, D.S., Swigon, D., Clermont, G.: A large-scale immuno-epidemiological simulation of influenza a epidemics. BMC public health **14**(1), 1–15 (2014)
29. Rahmandad, H., Sterman, J.: Heterogeneity and network structure in the dynamics of diffusion: Comparing agent-based and differential equation models. Management Science **54**(5), 998–1014 (2008)
30. Vlad, A.I., Sannikova, T.E., Romanyukha, A.A.: Transmission of acute respiratory infections in a city: Agent-based approach. Mathematical Biology and Bioinformatics **15**(2), 338–356 (2020)